

Impact of turbulence in long range quantum and classical communications

Ivan Capraro,¹ Andrea Tomaello,¹ Alberto Dall'Arche,¹ Francesca Gerlin,¹ Ruper Ursin,² Giuseppe Vallone,¹ and Paolo Villoresi¹

¹Department of Information Engineering, University of Padova, via Gradenigo 6/B

²Institute for Quantum Optics and Quantum Information (IQOQI),

Austrian Academy of Sciences, Boltzmannngasse 3, A-1090 Vienna, Austria

(Dated: August 27, 2018)

The study of the free-space distribution of quantum correlations is necessary for any future application of quantum as classical communication aiming to connect two remote locations. Here we study the propagation of a coherent laser beam over 143 Km (between Tenerife and La Palma Islands of the Canary archipelagos). By attenuating the beam we also studied the propagation at the single photon level. We investigated the statistic of arrival of the incoming photons and the scintillation of the beam. From the analysis of the data, we propose the exploitation of turbulence to improve the SNR of the signal.

PACS numbers: 03.67.Hk 42.50.Ar 92.60.Ta

Introduction - The study of the free-space propagation of quantum correlations is necessary for any future application of quantum communication aiming to connect two remote locations. The problem related to the free-space propagation is represented by the atmospheric turbulence, that acts as a temporal and spatial variation of the air refraction index. A turbulent channel acts an increment of the losses on the transmitted photons due to beam-wandering of the beam-centroid or scintillation, increasing the role of the noise [1–5]. The understanding of the propagation effects induced by turbulence at the receiver as well as the temporal statistics of the incoming photons is crucial to assess the quality of the communication and eventually the feasibility of the free-space ground-ground and space-ground links [6–8].

In this work we study the propagation of a free space optical link (143Km) between Tenerife and La Palma Islands of the Canary archipelagos [9–11]. The transmitter is located at La Palma, on the roof of the Jacobus Kapteyn Telescope (JKT) and the receiver is the Optical Ground Station (OGS) at Tenerife. The campaign was performed during the nights between 17 and 25 september 2011.

Optical Setup - The optical setup of the transmitter is shown in figure 1. It consists of suitably designed telescope whose key component is a singlet aspheric lens of 23 cm diameter and 220 cm focal length at 810nm. The lens diameter was chosen to be significantly greater of the estimated Fried parameter r_0 [12] in order to obtain a spot at OGS compared to the telescope primary mirror and consequently a greater power transfer between the two sites. Our light source is an infrared diode at 808nm coupled into single mode fiber with output power of about 6mW and suitable attenuators. In order to facilitate the raw pointing a mechanical XY stage has been added (we define the Z direction as the optical axis of the system). This stage moves all the 2.5m long telescope in the XY plane. All the structure is assembled by three aluminum flanges, one holds the lens, one the focal plane and the other is attached to the XY back stage. The lens is fixed to a articulated mount to prevent bending of the structure.

The IR source has been aligned by means of a dichroic mir-

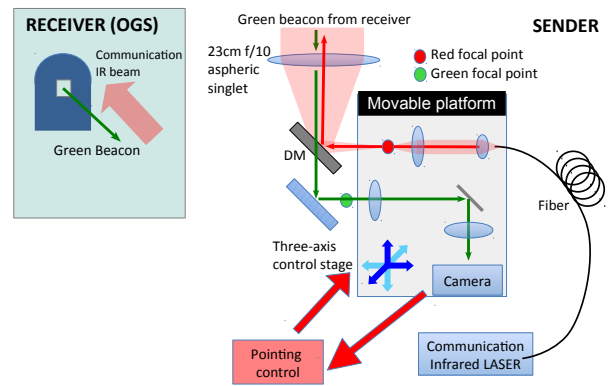


FIG. 1: Schematic of the optical setup.

ror (DM) reflecting the 808nm radiation. The platform carrying the focusing lens, the collimating lens and the fiber port for the IR can be moved by a micro metric XYZ system based on stepped motors. In this way the beam can be slightly steered by moving the focal spot at the singlet focus. The instantaneous deviation from the initial pointing direction is acquired by using a 532nm beacon beam sent from the receiver by using a small portable low power laser module directly pointed towards La Palma without any optics. The beacon laser is acquired with a CMOS camera placed on the movable platform after the DM transmission. The centroid of the beacon spot on the camera determines the correction on the outgoing IR laser by means of an error signal with respect to the reference position. The position of the spot at the camera are sampled about once a second and averaged for a number of frames and this data feeds a control software that calculates the movement for the fine XY stage in order to compensate slow drift in beam direction, which was performed in 1 sec timescale.

We collected data at the OGS in Tenerife in order to measure the received power, the scintillation and analyze the temporal structure of the signal. We placed in the OGS Coudé focus a photodiode, a power meter and, when the beam is

suitably attenuated with neutral filter, we also collected data with a single photon (Excelitas SPCM-AQRH model) detector (SPAD). The following data were recorded during the nights between 21th and the 24th September 2011. We obtained an average attenuation of about 30dB for many times during the best run with peaks of 27dB averaged over 2 minutes. The attenuation is calculated from the fiber and not from the singlet lens: the attenuation of the telescope is thus included in the measured attenuation.

Link Analysis - Let's first describe the single photon detection acquisition. We performed several measurements by setting the counting interval T to 0.1ms, 1ms and 10ms. Due to turbulence effects, the mean photon number q in a counting interval at the receiver should follow a lognormal probability distribution [13]:

$$P(q) = \frac{1}{q\sqrt{2\pi\sigma^2}} e^{-[(\ln \frac{q}{\langle q \rangle} + \frac{1}{2}\sigma^2)]^2 / (2\sigma^2)} \quad (1)$$

where $\langle q \rangle$ is the average, $\sigma^2 = \ln(1 + SI)$ and $SI = \frac{\Delta q^2}{\langle q \rangle^2}$ is the scintillation index. If the counting interval T is large compared with the coherence time of the source and T is short compared with the turbulence timescale, the probability of detecting n photon in each interval follow the Mandel distribution:

$$p_n = \int dq \frac{q^n e^{-q}}{n!} P(q) \quad (2)$$

Note that the mean number of detected photon is $\langle n \rangle = \sum_n n p_n = \langle q \rangle$. We report the analysis of the temporal distribution of an acquisition with 1ms counting interval in figure 2(top). It is possible to observe that, when the average number of detected photons, $\langle n \rangle$, is large (typically larger than 50) and the scintillation index bigger than 1, the lognormal and Mandel distribution are quite similar. Given the experimental scintillation as 2.23 ± 0.01 and the mean value of detected photon as 234, we show the counting occurrences together with the corresponding lognormal distribution in figure 2(bottom). For comparison, we also insert the corresponding Mandel distribution with the $\langle q \rangle = 234.1 \pm 0.1$ and $\sigma = 349.2 \pm 0.2$ parameter obtained from the raw data. We evaluated the similarity between the experimental data and the lognormal or the Mandel curve, defined as $S = \frac{(\sum \sqrt{p_i q_i})^2}{\sum p_i \sum q_i}$ where p_i and q_i are respectively the theoretical and experimental occurrence. The similarity of the lognormal curve with the data is 0.9959 while the Mandel curve has a similarity of 0.9967 showing a clear evidence of the statistic transformation. The green curve represents the corresponding Poisson distribution with the same observed mean value, to compare what it have been obtained if the statistic of arrival photon would be purely poissonian. In table I we report the data obtained for several different SPAD acquisitions.

As said, we also measure the intensity of received light with a fast photodiode by using an intense laser source. In figure 3 we plot the temporal distribution of the photodiode voltage of a data set covering 20 s. The intensities are recorded

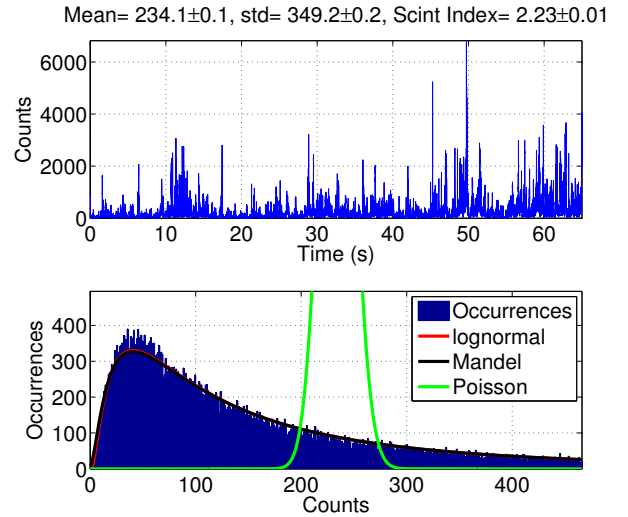


FIG. 2: SPAD temporal distribution of count occurrences and corresponding lognormal and Mandel curves. We can compare the data with the corresponding Poissonian distribution with the same mean value (234.1 ± 0.1) that would be obtained without turbulence.

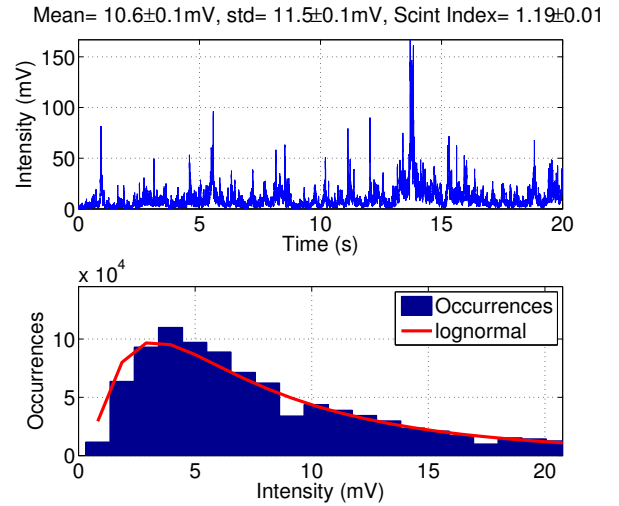


FIG. 3: Photodiode temporal distribution intensity occurrences and corresponding lognormal curve.

with 50kHz frequency. Also in this case the intensity occurrences follows a lognormal distribution (1) as shown from the lognormal curve with similarity of 0.9896. In this case the scintillation index evaluated from the experimental data is $SI = \frac{\Delta I^2}{\langle I \rangle^2} = 1.19 \pm 0.01$.

Improving the SNR - For both quantum and classical communication, it is of paramount importance achieving an high signal to noise ratio (SNR). If a qubit state $|\psi\rangle$ encoded in the photon polarization must be sent between two remote location, it is possible to determine the effect of (white) noise on the polarization fidelity[14]. Let's measure the SNR in dB, namely $SNR = 10 \log_{10} \frac{N_s}{N_n}$, where N_n the average amount of

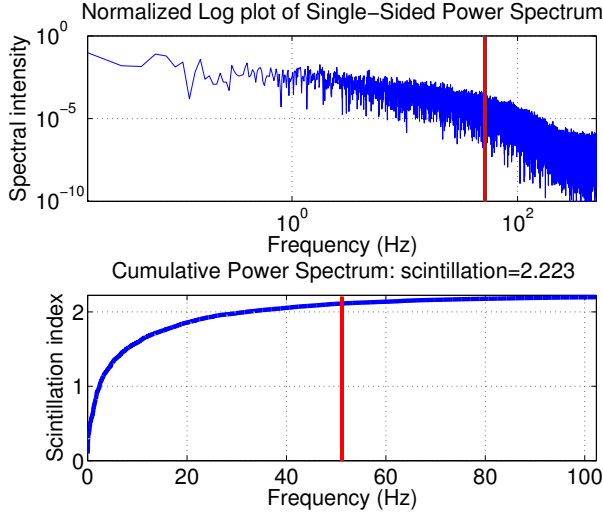


FIG. 4: SPAD power spectrum and cumulative power spectrum. Frequency bound (red line): the frequencies below 51.1724 Hz contribute to the 95% of the scintillation index.

noise (coming from dark detections or background radiation) and N_s is the average counting signal. It is easy to show that the fidelity depends on the SNR as:

$$F = 1 - \frac{1}{1 + 10^{SNR/10}}. \quad (3)$$

In order to improve the SNR for the transmission of single photons in a long distance free-space link as the present one which use a 1m optical receiver, out of our findings we envisage the exploitation of the following procedure. With a given frequency (slower than the single photon transmission rate) the free-space channel is probed by means of a classical signal that gives the information of the instantaneous transmission of the channel. Only if the transmission is above a given threshold the single photon signal is acquired. It is crucial for the protocol to be efficient to correctly identify the "probing" frequency and the threshold to be used. This technique can be also used in the classical case, for instance in the on-off keying.

We report in figure 4 the frequency spectrum and the cumulative power spectrum of the data plotted in figure 2. The normalized plot of the power spectrum is obtained by normalizing the intensities by the average $I' = I/\langle I \rangle$. The power spectrum is related to the scintillation index as follow. We write the set of (normalized) acquisitions as I'_k with $k = 0, \dots, N-1$ and $N = 20s/20\mu s = 10^6$ the number of intensity acquisitions over the 20 seconds. The Fourier components are given by $\tilde{I}_n = \sum_k I'_k \omega^{nk}$ with $\omega = e^{-\frac{2\pi i}{N}}$. By Parseval's theorem it is easy to show that $SI = \frac{2}{N^2} \sum_{n=1}^{N/2} |\tilde{I}_n|^2$, namely it is the cumulative power spectrum without the zero frequency (\tilde{I}_0) component. We can notice that the frequencies contributing to the scintillation (up to 95%) are within (almost) 50Hz. For frequencies above around 500Hz, the spectrum becomes flat, indicating that at this frequency the random noise is domi-

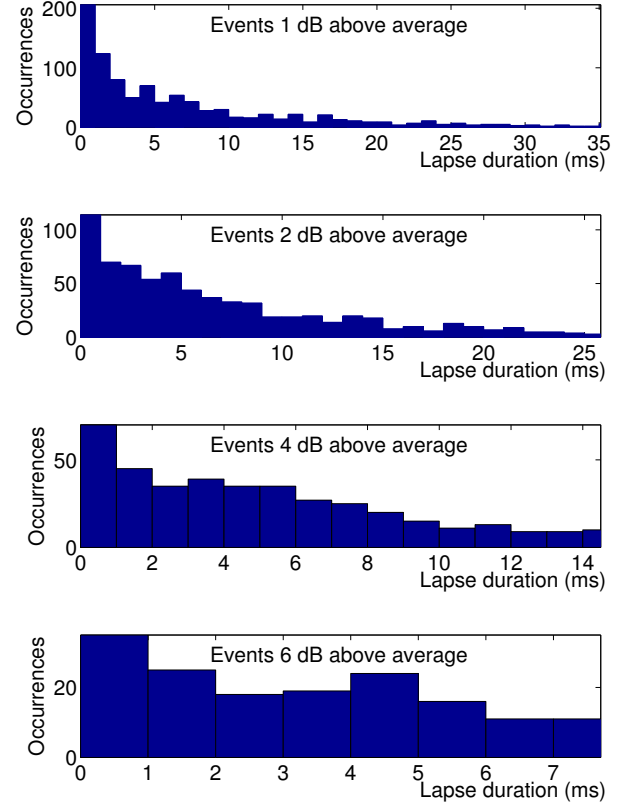


FIG. 5: Duration (in ms) of events with over-threshold counting: in the different plots we considered a threshold of 1, 2, 4 and 6 dB above the average.

nant. The typical fluctuations of the transmission channel due to turbulence are within 100Hz (see table I). The frequency analysis of the temporal scintillation indicates that the probing frequency doesn't need to be higher than 1KHz.

In order to obtain a further evidence, we analysed the features of the counts above a given threshold of the signal reported in fig. 2. By considering a threshold of 1, 2, 4 and 6 dB above the average we considered the duration (in ms) of events with over-threshold counting. The results are shown in figure 5. The probability of obtaining an event above a given threshold q_0 can be predicted from the lognormal distribution[15]

$$p(q > q_0) = \frac{1}{2} - \frac{1}{2} \operatorname{erf} \left[\frac{\ln \frac{q_0}{\langle q \rangle} + \frac{1}{2} \sigma^2}{\sqrt{2} \sigma^2} \right] \quad (4)$$

where $\operatorname{erf}(x)$ is the Gaussian error function $\operatorname{erf}(x) = \frac{2}{\sqrt{\pi}} \int_0^x e^{-t^2} dt$. Acquiring the single photon channel only if the "probed" transmission is above a given threshold implies an increase of the average photon counts in each time-slot. It is possible to show that, by considering only the events in which the transmission satisfy $T > T_0$, the new mean value $\langle n \rangle_{thres}$ is

$$\frac{\langle n \rangle_{thres}}{\langle n \rangle} = \frac{1 - \operatorname{erf} \left[\frac{\ln \frac{T_0}{\langle T \rangle} - \frac{1}{2} \sigma^2}{\sqrt{2} \sigma^2} \right]}{1 - \operatorname{erf} \left[\frac{\ln \frac{T_0}{\langle T \rangle} + \frac{1}{2} \sigma^2}{\sqrt{2} \sigma^2} \right]} > 1 \quad (5)$$

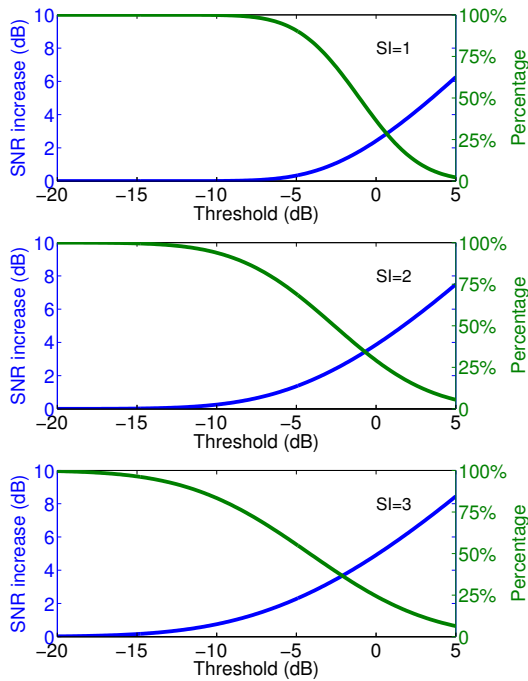


FIG. 6: SNR and the percentage of the overall counts that will be detected in function of the threshold selection.

Clearly, this threshold selection increase the SNR, but at the same time decrease the overall counts in given time. In figure 6 we show the increase (in dB) of the SNR and the percentage of the overall counts that will be detected. In cases of strong turbulence and high noise, this technique could help the qubit transmission by "exploiting turbulence", namely considering only the particular moments in which the turbulence increase the channel transmission.

In conclusion, the statistic of arrival of single photon over free-space 143Km optical link has been analyzed demonstrating the transformation from Poissonian to Lognormal distribution thus expanding this investigation for more than an order of magnitude in length with respect to previous results [13]. The evidence of consecutive subintervals of low losses allows to envisage the exploitation of turbulence as an SNR improvement technique.

The authors wish to thank the staff of IAC: F. Sanchez-Martinez, A. Alonso, C. Warden, M. Serra, J. Carlos and the staff of ING: M. Balcells, C. Benn, J. Rey, O. Vaduvescu, A. Chopping, D. González, S. Rodríguez, M. Abreu, L. González; J. Kuusela, E. Wille, as well as Z. Sodnik, and J. Perdígues of the OGS of ESA. This work has been carried out within the Strategic-Research-Project QUINTET of the Department of Information Engineering, University of Padova and the Strategic-Research-Project QUANTUMFUTURE of the University of Padova.

	Mean	Std	Time(s)	Window (ms)	SI	Bound(Hz)
backgr.	0.4732	0.7256	10	1	2.3515	475
Hi	5291	9135	650	10	2.9805	22
Hi	678.7	820.8	65	1	1.4626	43
Hi	510.4	751.9	65	1	2.1704	45
Hi	781.5	951.9	65	1	1.4834	42
Hi	180.2	312.0	65	1	2.997	39
Hi	234.1	349.2	65	1	2.2251	51
Hi	43.18	48.76	6.5	0.1	1.2748	81
Hi	21.17	26.34	6.5	0.1	1.5485	88
Hi	75.37	132.10	6.5	0.1	3.072	35
Hi	59.97	105.01	6.5	0.1	3.0659	37
Low	37.86	48.42	200	10	1.6355	35
Low	20.83	24.18	200	10	1.3479	35
Low	2.862	3.795	65	1	1.7578	384
Low	5.267	7.519	65	1	2.0383	258

TABLE I: Data obtained for different single photon acquisition compared to the background (first line). For each acquisition we report the total duration of the acquisition (Time), the temporal windows defining the counting interval (Window), the mean number of counts in the counting interval (Mean) and its the standard deviation (Std). We also report the scintillation index (SI) and the frequency bound such that all the frequencies below the bound contribute up to 95% of the scintillation (Bound). With High (Low) we indicate acquisition with high (low) mean photon number detected during 1s. We notice that for the last two data sets the bound is higher due to the low signal compared to the background (having flat frequency spectrum).

-
- [1] V. I. Tatarski, *Wave Propagation in a Turbulent Medium* (McGraw-Hill, 1961).
 - [2] R. L. Fante, Proc. IEEE **63**, 1669 (1975).
 - [3] R. Fante, IEEE Trans Antennas Propagat. **AP-23**, 382 (1975).
 - [4] R. L. Fante, Proc. IEEE **68**, 1424 (1980).
 - [5] F. Dios, J. A. Rubio, A. Rodríguez, and A. Comerón, Applied optics **43**, 3866 (2004), ISSN 0003-6935.
 - [6] P. Villoresi, T. Jennewein, F. Tamburini, M. Aspelmeyer, C. Bonato, R. Ursin, C. Pernechele, V. Luceri, G. Bianco, A. Zeilinger, et al., New Journal of Physics **10**, 033038 (2008), ISSN 1367-2630.
 - [7] C. Bonato, A. Tomaello, V. Da Deppo, G. Naletto, and P. Villoresi, New Journal of Physics **11**, 045017 (2009), ISSN 1367-2630.
 - [8] E. Meyer-Scott, Z. Yan, A. MacDonald, J.-P. Bourgoin, H. Hübel, and T. Jennewein, Physical Review A **84**, 1 (2011), ISSN 1050-2947.
 - [9] R. Ursin, S. Backus, H. C. K. F. Tiefenbacher, T. Schmitt-Manderbach, H. Weier, T. Scheidl, M. Lindenthal, B. Blauensteiner, T. Jennewein, J. Perdígues, et al., Nature Physics **3**, 481 (2007).
 - [10] A. Fedrizzi, R. Ursin, T. Herbst, M. Nespola, R. Prevedel, T. Scheidl, F. Tiefenbacher, T. Jennewein, and A. Zeilinger, Nature Physics **5**, 389 (2009).
 - [11] T. Scheidl, R. Ursin, J. Kofler, S. Ramelow, X.-S. Ma, T. Herbst, L. Ratschbacher, A. Fedrizzi, N. K. Langford, T. Jennewein, et al., Proc. Natl. Acad. Sci. USA **107**, 19708 (2010).

- [12] D. L. Fried, *Journal of the Optical Society of America* **56**, 1372 (1966).
- [13] P. W. Milonni, J. H. Carter, C. G. Peterson, and R. J. Hughes, *Journal of Optics B: Quantum and Semiclassical Optics* **6**, S742 (2004), ISSN 1464-4266.
- [14] If $|\psi\rangle$ is the polarization state of the sent photon and ρ is the polarization density matrix of the received photon, the fidelity $F = \langle\phi|\rho|\phi\rangle$ is the probability of receiving the correct state.
- [15] Here we replaced the Mandel distribution with the lognormal distribution.